Lyudmila Nyrkova, Pavlo Lisovyi, Larysa Gonchasrenko, Svetlana Osadchuk, Yulia Kharchenko, Anatoly Klymenko, Valery Kostin*

E.O. Paton Electric Welding Institute of the National academy of sciences of Ukraine, Kyiv, Ukraine

Scientific paper
ISSN 0351-9465, E-ISSN 2466-2585
https://doi.org/10.5937/zasmat2301096N

Zastita Materijala 64 (1)
96 - 106 (2023)

Investigation of stress-corrosion cracking of welded joint of X70 steel under cathodic polarization in near neutral environment

ABSTRACT

Study of stress-corrosion cracking of welded joints made of X70 steel at cathodic polarization in near neutral solution NS4 was carried out. It was established that the tendency of base metal of X70 steel to stress-corrosion cracking, estimated by K_S coefficient, increases from 1.07 to 1.13 whereas polarization potential changing from the corrosion potential to maximum protective potential -1.05 V. Such regularity correlates with increasing of hydrogen penetration through X70 steel, which at maximum protective potential -1.05 V is equal to 0.000518 mol/m^3. Susceptibility of welded joint is lower than the base metal, K_S coefficient change not much near the value 1.0. With increasing of polarization potential from -0,75V to -1.05V fracture surface of X70 steel characterized by decreasing in the size of holes and the appearance of flat areas, through that the rupture occurred. A similar nature of the rupture was observed for the welded joint, but visually larger proportion of flat areas can be noted. It was established that the rupture of the welded joint occurs on the base metal, which allows to propose stress-corrosion cracking susceptibility factor K_S to be legitimately used for estimation to stress-corrosion cracking of welded joint, provided the weld is performed in a high-quality manner. Stress-corrosion cracking results of welded joint of X70 steel correlate satisfactorily with the experience of stress-corrosion cracking on main gas pipelines, where stress-corrosion cracks form and develop along the base metal of gas pipelines.

***Keywords**: pipe steel X70, welded joint, near-neutral environment, cathodic polarization, stress-corrosion cracking, slow strain rate test, voltammetry, fractography*

1. INTRODUCTION

Main gas pipelines are the main type of gas transportation in the modern world, and their safety and reliability of operation has significant influence on the development of state's economy. During the last decades, many studies focused mainly on various factors of stress-corrosion cracking (SCC) of high and medium strength pipe steel in soil conditions at cathodic protection [1-5]. SCC of underground pipelines during operation is one of the biggest hidden causes of their destruction. Under the influence of the external environment, SCC mainly proceeds by different mechanisms: at high pH – by the mechanism of intercrystalline cracking [6,7], at near neutral pH – by transcrystalline cracking [8, 9]. Due to the fact that pipelines are in operation for a long time, damages of the protective coating of pipeline and the formation of defects in it under combined action of applied potential and the soil environment is a common phenomenon, which leads to serious risks of SCC in environments. SCC studies in laboratory conditions are usually carried out by slow strain rate method. Many studies are devoted to the study of stress-corrosion cracking of pipe steels, for example X65, X70, X80 [10-15] in near neutral and alkaline environments. But there is quite limited data on SCC of welded joints.

In [16] it is shown that both X90 pipe steel and its welded joint under cathodic polarization are susceptible to SCC by the mechanism of intergranular cracking. In the range of potentials from the corrosion potential to -1000 mV, the SCC mechanism of both X90 steel and its welded joint is combined – anodic dissolution (AD) and hydrogen embrittlement (HE). At the corrosion potential, the susceptibility to SCC is due to the strong effect of anodic dissolution. At -800 mV susceptibility to

Corresponding author: Lyudmila Nyrkova
E-mail: lnyrkova@gmail.com, nyrkova@paton.keiv.ua
Paper received: 20. 08. 2022.
Paper accepted: 29. 09. 2022.
Paper is available on the website: www.idk.org.rs/journal

SCC reduces due to weaker AD and HE, and increases significantly at -900 mV due to increasing effect of hydrogenation. The SCC tendency of the weld is higher than that of the base metal, which may be related to the phase transformation of the structure in the seam during welding.

In [17] it was established that the sensitivity of the heat affected zone (HAZ) to SCC depends on two factors: the influence of the microstructure in the HAZ on electrochemical reactions and the influence of mechanical stress on the initiation of stress corrosion cracks. The SCC behavior is consistent with the electrochemical results: at a potential of −650 and −850 mV, SCC is most likely to occur in the softened region, and below −1200 mV it occurs in both the softened and hardened regions.

For X90 steel and its welded joint, the existence of three SCC mechanisms was established in [18]: the mechanism of anodic dissolution at the corrosion potential, anodic dissolution and hydrogen cracking at the potential of -850 mV, and the mechanism of hydrogen embrittlement at the applied potential of -1000 mV and -1200 mV.

In welded joint made of X70 steel in a near-neutral solution, the susceptibility to SCC increases with decreasing potential, but when the potential is too negative, the susceptibility to SCC decreases. In addition, with decreasing pH and an increasing of corrosion rate of steel, the potential range in which the SCC develops becomes more negative. From the analysis of the SCC mechanism, it was determined that in HAZ of the samples, hydrogen cracking occurs together with anodic dissolution [19].

The influence of the oscillation frequency on SCC of welded joint of X70 pipe steel was studied under cathodic polarization in near-neutral pH environment by slow strain rate fluctuating method. Susceptibility to SCC occurs in HAZ of the welded joint of X70 steel with cathodic polarization. An SCC crack can appear due to microdefects on the surface of the material and spread as the main stress spreads over the surface, when the frequency of its fluctuations increases to a certain level, the SCC crack spreads along the plane of maximum shear stress [20].

The article [21] investigated the influence of pre-plastic deformation on corrosion cracking susceptibility of a welded joint made of X70 steel with near-neutral pH using a slow strain rate tensile test. Generally, pre-plastic deformation reduces SCC resistance in different weld zones. Susceptibility of the examined zones of the welded joint to SCC can be arranged in the following order: HAZ > weld metal > base metal. Fractographic analysis showed that there are two modes of cracking. Type I cracks propagate along the direction perpendicular to the maximum tensile stress, while type II cracks lie in planes approximately parallel to the plane of maximum shear. The SCC of the base metal and HAZ is governed by type I cracking, while the weld is dominated by type II cracking. The increased susceptibility to SCC caused by prior plastic deformation may be associated with an increase in yield strength.

Therefore, there is some inconsistency in the data on SCC of welded joints. From our experience of analysis of destruction due to SCC of main gas pipelines [22] it is known that stress-corrosion cracks occur at the distance 20-25 mm from the longitudinal weld, that is, on the base metal. Therefore, the purpose of the work was to study of stress-corrosion cracking of welded joints made of X70 steel at cathodic polarization in near neutral environment.

2. EXPERIMENTAL

The research was carried out in the model soil electrolyte NS4, which is usually used to study stress-corrosion cracking. Its chemical composition, g/l: 0.122 KCl + 0.483 $NaHCO_3$ + 0.181 $CaCl_2$ + 0.131 $MgSO_4$ [23].

Research objects are low-alloy steel X70 of the pipe assortment and its welded joint. Chemical composition of X70 steel and the weld is presented in Table 1.

Table 1. Chemical composition of base metal of X70 steel and the weld

Tabela 1. Hemijski sastav osnovnog metala čelika X70 i vara

Specimen characteristic	*C*	*Mn*	*Si*	*S*	*P*	*Al*	*Ni*	*Mo*	*Ti*	*V*	*Nb*
Base metal of X70 steel	0,096	1,71	0,208	0,009	0,007	0,035	0,03	0,03	0,015	0,06	0,052
Weld	0,08	1,37	0,57	0,019	0,024	0.01	0.06	0,15	0.005	0.02	0.01

Table 2. Mechanical properties of base metal of X70 steel and its welded joint

Tabela 2. Mehanička svojstva osnovnog metala čelika X70 i njegovog zavarenog spoja

Specimen characteristic	$\sigma_{0,2}$, MPa	σ_B, MPa	δ_5, %
Base metal of X70 steel	440	590	20
Welded joint	504	606	22,4

Templates made of X70 steel with a thickness 16 mm and a size of 15.5×200×750 mm were welded by four-arc welding with Sv-08G1HMA wire, with diameter 4 mm under OP 132. Welding mode (arc feeding from a rectifier VSZH-1600, reverse polarity): for internal weld I =650 A, U=37.5V; external weld I=800 A, U=37-38V, electrode slope 5°. Welding speed 24.7 m/h, forward angle. The size of the outer weld is 14×27×2.5 mm, the inner weld is (5.5-6) ×26×3.0 mm, the overlap of the welds was from 4 to 4.5 mm.

Since stress-corrosion cracking during the operation of underground gas pipelines occurs from the outer surface, which is under cathodic protection, the samples were polished minimally from the side of the facing (external) seam. Specimens for electrochemical and slow strain rate investigation was cutted from the steel plate and from the welded joint template.

Corrosion-mechanical studies were carried out by slow strain rate method with the speed 10^{-6} s^{-1} on the AIMA-5-1 machine in NS4 solution with periodic immersion: 50 minutes in the solution, 10 minutes in air [24]. The shape and dimensions of the samples are shown in **Fig. 1**. Some of the specimens were subjected to cathodic polarization at protective potential -0.75, -0.95 and -1.05V (respectively -0.85, -1.05 and -1.15V relative to the copper sulfate electrode according to DSTU 4219), which simulated the conditions of the cathodic protection on underground gas pipeline.

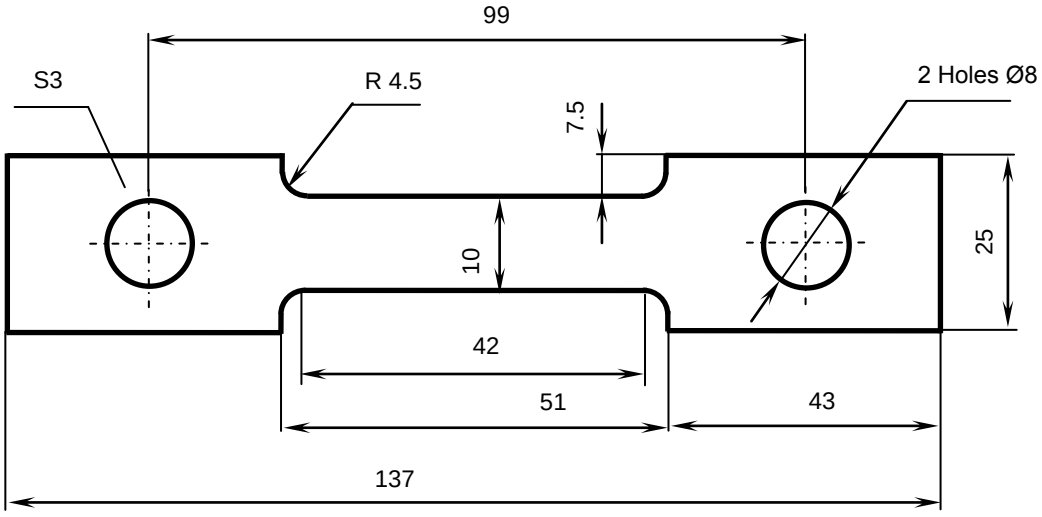

Figure 1. Specimen sketch for corrosion-mechanical tests at low strain rate method [25]

Slika 1. Skica uzorka za koroziono-mehanička ispitivanja metodom niske brzine deformacije [25]

Electrochemical studies were carried out on a pressing electrochemical cell, the design of which allows measurements to be performed on different zones of welded joint, according to the three-electrode scheme in potentiodynamic mode using PI-50-1.1 potentiostat and PR8 programmer. The potentials were measured relative to silver chloride reference electrode (s.c.e.). Polarization curves were recorded with a potential sweep speed 10^{-3} V/s. The curves were taken on the base metal of X70 steel and on the weld. Platinum electrode were used as an auxiliary electrode. The research results were presented in semi-logarithmic coordinates "lg i - E", where i is the current density per unit surface area of the sample in A/m^2, E is the potential in Volts. Electrochemical parameters were determined from the polarization curves using a graphic-analytical method.

Grits for metallographic studies were made according to standard methods. Microstructure of samples was detected by etching in nital (solution of 4% nitric acid in ethyl alcohol) and studied using a NEOPHOT 21 microscope. A digital image of the microstructure of the samples was obtained using an Allied Vision 1800 U-2050c digital camera and SEOimageLAB software. Examination of the

surface of the samples after rupture was carried out on a JSM 840 scanning electron microscope (JEOL, Japan) in the mode of secondary and backscattered electrons at an accelerating voltage of 20 kV and an electron beam current (10^{-7}-10^{-10}) A at different magnifications (from ×12 to ×500).

The susceptibility of steel to hydrogenation was investigated according to the GOST R 9.915 methodology [26] on laboratory setup that has two separate chambers: oxidation chamber and chamber for hydrogenation. In the oxidation chamber, an anodic potential was set on the working electrode surface, after reaching its constant value, the investigated solution was introduced into the irrigation chamber and a cathodic potential was set in the range from -0.85V to -1.05 V. A 0.1 M NaOH solution was used in the anodic chamber, in the cathode - model soil electrolyte NS4. The concentration of hydrogen penetrating the steel was calculated according to the formula:

$$J_{st} = \frac{I_{st}}{FS} = \frac{DC_0}{L}, \qquad (1)$$

Where

J_{st} – flow of hydrogen penetration into the surface layer of X70 steel on the oxidized side of the membrane at steady state, mol/(m^2·s);

I_{st} – current strength in the stationary mode of hydrogen penetration, A;

S – area of studied sample, m^2;

F – Faradey constant, Kl/mol;

D – diffusion coefficient of hydrogen equal $1{,}5\cdot10^{-5}$ cm^2/s;

C_0 – hydrogen concentration in the surface layer of the steel from the side of the hydrogenation chamber, mol/m^3;

L – membrane (specimen) thickness, m

Current strength in the stationary mode of hydrogen penetration is calculated according to the equation:

$$I_{st} = I_{H_2} - I_B, \qquad (2)$$

Where

I_{H_2} – total amperage measured in the oxidation chamber, A;

I_B – background current, A.

The concentration of hydrogen penetrating into the surface layer of steel was calculated by the formula:

$$C_0 == \frac{I_{st}\cdot L}{D_{H_2} FS} \qquad (3)$$

3. EXPERIMENTAL RESULTS

3.1. Microstructure of X70 steel and welded joint

X70 steel has a dispersed ferrite-pearlite structure with grain elongation in the rolling direction (Fig. 2, a). The ferrite grain corresponds to the (10-11) number according to DSTU 8972 [27], the banding of the metal is (3-4) points, row B according to GOST 5640. The hardness of the steel is within (180-190) HV_5.

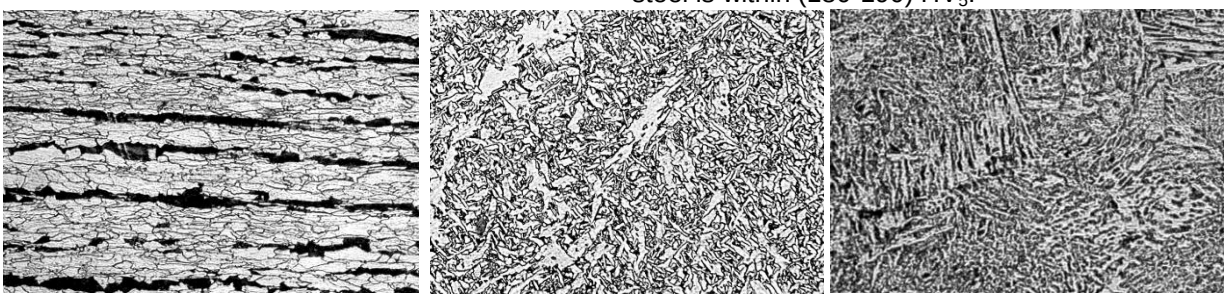

a) b) c)

Figure 2. Microstructure of the base metal of X70 steel, ×400 (a), of the external weld, ×400 (b); of the coarse grain zone, ×400 (c)

Slika 2. Mikrostruktura osnovnog metala čelika X70, x400 (a), spoljašnjeg šava, x400 (b); zone krupnog zrna, x400 (c)

Microstructure of the external seam metal of welded joint is dispersed acicular ferrite with intergranular pre-eutectoid ferrite allocations in the form of thin continuous layers, individual grains, and individual coarse conglomerates of the so-called massive pre-eutectoid ferrite (Fig. 2, b, c). The part of pre-eutectoid polygonal ferrite in the metal of weld does not exceed 6%.

In heat affected zone (HAZ) on the coarse grain area, the structure is bainite-type (ferrite with second-phase discharges, mainly of lamellar morphology) with formations of polygonal pre-

eutectoid ferrite formations on the boundaries of past austenite grains (Fig. 2, c). The size of coarse grain in HAZ in the area adjacent to the fusion line, is number 4, according to DSTU 8972 [27].

3.2. Electrochemical investigation of welded joint of X70 steel

Corrosion potential of the weld is more positive than the potential of base metal X70 steel (Fig. 3, a), but difference between corrosion potential of base metal and weld seam is 12 mV, Table 3, which, according to GOST 9.005 [28] does not dangerous (because of potential difference more than 50 mV is considered dangerous for welded joints) and can be expected not to lead to predominant corrosion of weld.

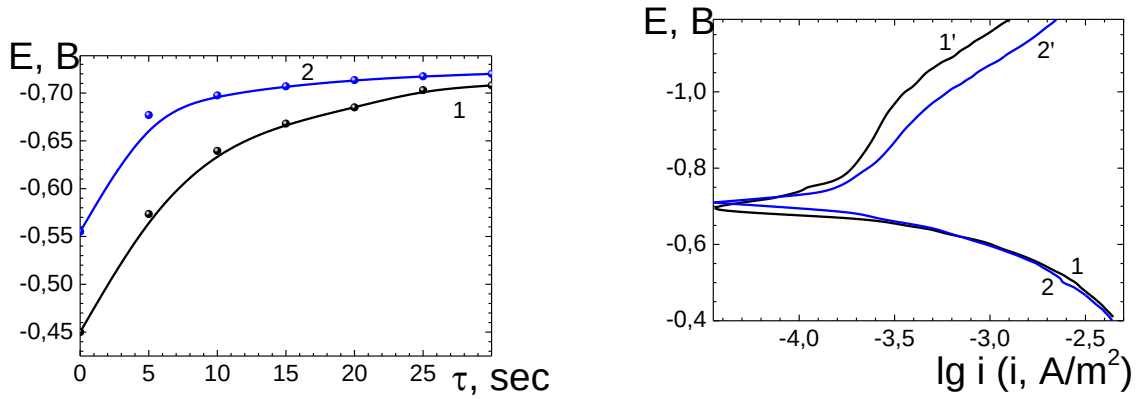

a) b)

Figure 3. Corrosion potentials (a) and polarization curves (b) of base metal (1, 1') of X70 steel and weld (2, 2'): 1, 2 – anodic curves; 1', 2' – cathode curves

Slika 3. Potencijali korozije (a) i polarizacione krive (b) osnovnog metala (1, 1') čelika X70 i šava (2, 2'): 1, 2 – anodne krive; 1', 2' – katodne krive

Table 3. Electrochemical characteristics of base metal and weld of X70 steel in NS4

Tabela 3. Elektrohemijske karakteristike osnovnog metala i vara od čelika X70 u NS4

Welded joint zone	E_{cor}, V	**Electrochemical characteristics of processes**			
		anodic	**cathodic**		
		b_a, V	i, A/m^2	i_d, A/m^2	E_{H2}, V
Base metal	-0,720	0,057	$7.9 \cdot 10^{-5}$	$2.45 \cdot 10^{-4}$	-0,99
Weld	-0,708	0,038	$1.9 \cdot 10^{-4}$	$3.24 \cdot 10^{-4}$	-0,93

Notes. E_{cor}- corrosion potential; b_a - anodic polarization curve slope; i - anodic current density at potential -0,64 B; i_d - density of the limit diffusion current of oxygen reduction; E_{H2}- hydrogen reduction potential

The nature of the anodic and cathodic polarization curves both the base metal and weld is the same (Fig. 3, b). In the potentials area, located from the corrosion potential to -0.66V, currents on weld seam are greater than on the base metal, at more positive potentials, both curves coincide. For example, at -0.680V, the anodic dissolution currents of weld are an order of magnitude higher than currents for the base metal, Table 1.

The slope of anodic curve for the base metal is 0.057 V, for the weld seam is 0.038V, i.e. corrosion process goes with diffusion control, but on the weld seam it is complicated, probably by surface passivation, caused by the presence of alloying elements in the seam.

The limiting current of oxygen reduction on the base metal is 1.3 times less than on the weld (Table 3). With free access of oxygen in aqueous solutions, corrosion occurs with diffusion control, therefore, higher oxygen recovery current at the weld will help accelerate the corrosion process.

The hydrogen recovery potential on the weld seam is slightly lower in absolute value compared to the base metal (Table 3). Of course, this can create conditions for preferential flooding of the weld area.

3.3. Stress-corrosion cracking investigation

Assessment of susceptibility to stress-corrosion cracking was carried out both by indicators of changes in corrosion-mechanical properties and by changes in the nature of destruction. In previous works [29,30] we proposed the dimensionless coefficient K_S for estimating the degree of susceptibility to stress-corrosion cracking:

$$K_S = \frac{\psi_{air}}{\psi_{sol}}, \quad (4)$$

ψ_{air}, ψ_{sol} - relative shrinkage of samples in air and in solution, respectively

This coefficient was successfully used to assess the susceptibility to SCC of steels of different chemical composition, namely 09G2S, 17G1S, X70 [25,31,32]. In this work, one of the tasks was to investigate the legality of its using for assessing the susceptibility to SCC of a welded joint.

Breaking diagrams of X70 steel and welded joint under different conditions are shown in Fig. 4. It is natural that rupture of welded samples (Fig. 4, b) occurred at lower relative elongation than rupture of the base metal. In corrosive environment, the process of breaking both the base metal and welded joints occurs faster than in air, and the applying of cathodic polarization accelerated this process even more and changed its character, Fig. 4.

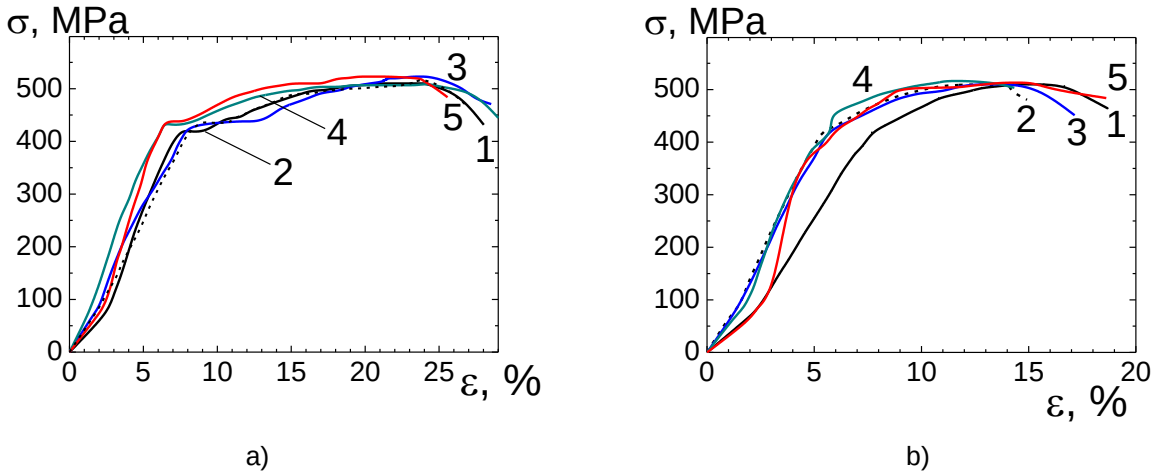

a) b)

Figure 4. Breaking diagrams X70 steel samples (a) and welded joints (b) during corrosion-mechanical tests in air (1), in NS4 solution under different conditions: 2 – at corrosion potential; at polarization potentials, 3 – -0.75 V; 4 – -0.95 V; 5 – -1.05 V

Slika 4. Dijagrami lomljenja uzoraka čelika X70 (a) i zavarenih spojeva (b) tokom koroziono-mehaničkih ispitivanja na vazduhu (1), u rastvoru NS4 pod različitim uslovima: 2 – pri potencijalu korozije; na polarizacionim potencijalima, 3 – -0,75 V; 4 – -0,95 V; 5 – -1,05 V

Air-breaking samples of X70 steel and welded joint have all the signs of ductile failure: indentation near fracture region, the presence of areas that have undergone plastic deformation. Decreasing in the relative elongation of welded joint compared to base metal by almost 33% was noted. In the morphology of fractures of the base metal and welded joints, viscous (holes) character prevails (Fig. 5,6), but character of welded joint morphology is characterized by a smaller diameter and depth of holes.

After tests in NS4 solution without polarization, that is, at corrosion potential, the nature of destruction of the base metal and welded joint remains viscous. Compared to specimens, tested in air, the relative elongation of the base metal decreased by 4% (from 28.0 to 27.0%), and the relative narrowing decreased by 7% (from 53.1 to 49.3%), Table 4. The coefficient of susceptibility to stress-corrosion cracking was equal to 1.07, Fig. 7 (curve 1), a viscous (dimpled) character prevails in the morphology of the fracture (Fig. 5). For the welded joint, the relative elongation decreased more strongly, by 9% (from 18.7 to 17.1%), Fig. 4, a, relative narrowing by 17% (from 42.7 to 35.2%). The coefficient of susceptibility to stress-corrosion cracking was equal to 1.21, Fig. 7 (curve 2). The nature of the morphology of the base metal and the welded joint is similar to the morphology, that observed for the samples breaking in air (Fig. 5, 6).

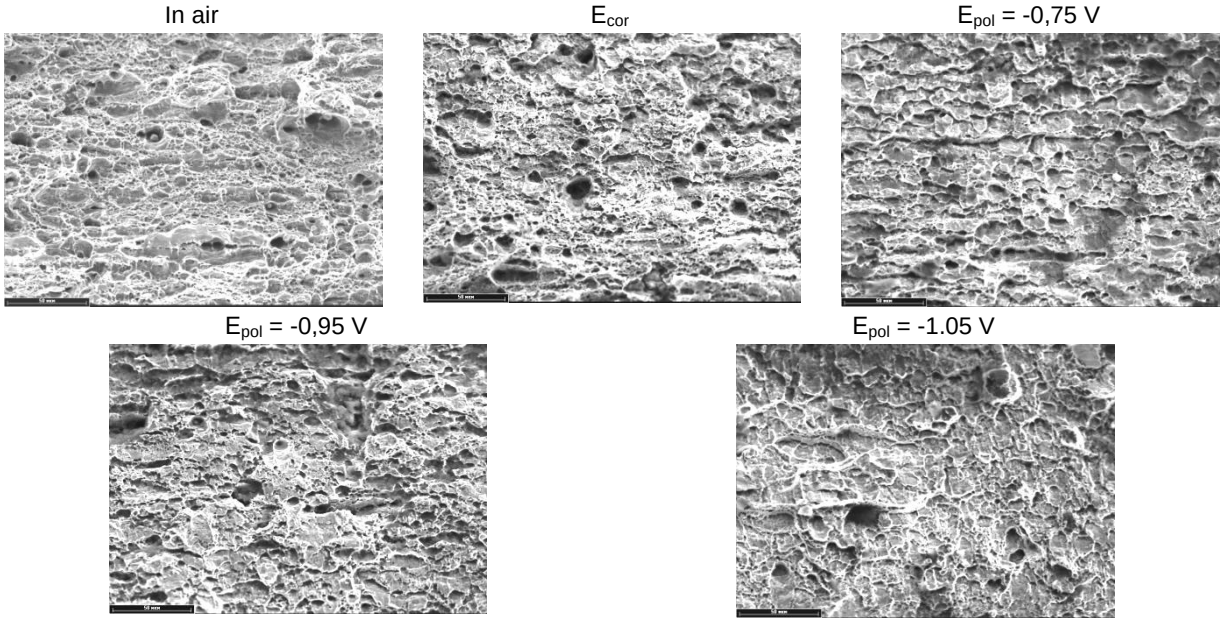

Figure 5. Fracture surfaces of X70 steel samples after corrosion-mechanical tests in air and in NS4 solution under different conditions

Slika 5. Površine loma uzoraka čelika X70 nakon koroziono-mehaničkih ispitivanja na vazduhu i u rastvoru NS4 pod različitim uslovima

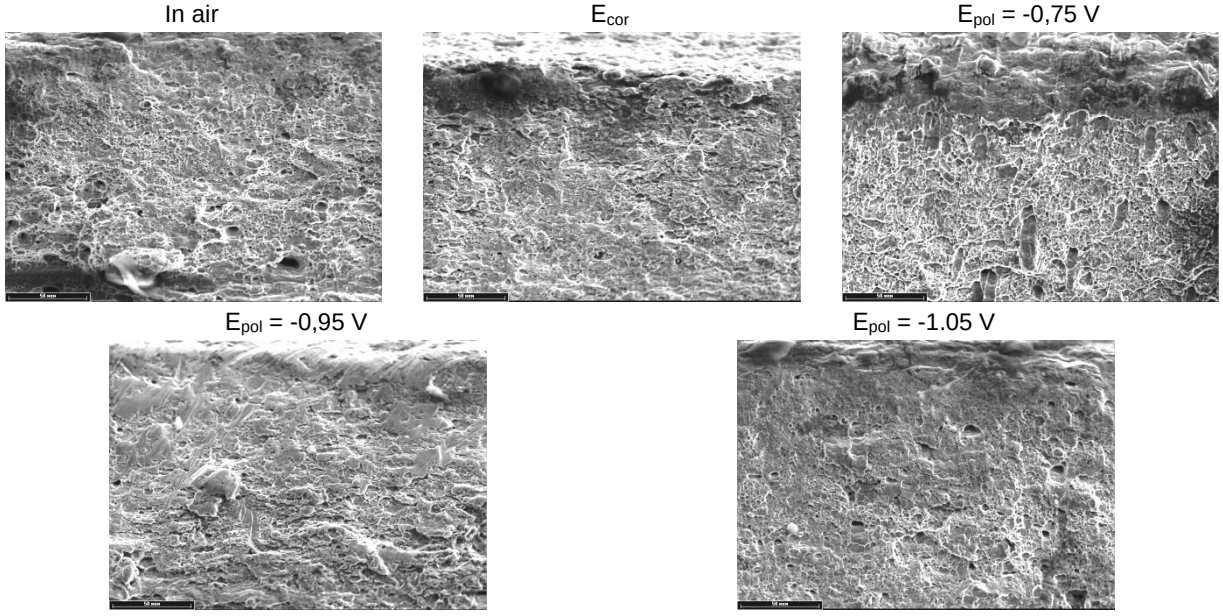

Figure 6. Fracture surfaces of welded joints if X70 steel samples after corrosion-mechanical tests in air and in NS4 solution under different conditions

Slika 6. Površine loma zavarenih spojeva u uzorcima čelika X70 nakon koroziono-mehaničkih ispitivanja na vazduhu i u rastvoru NS4 pod različitim uslovima

At the minimum protective potential of -0.75V, the destruction of the base metal also occurred mainly viscously. Relative elongation compared to air slightly increased, probably within the scatter range (from 28.0 to 28.5%), Fig. 4. The relative narrowing increased by 4% (Table 4), the coefficient of susceptibility to stress-corrosion cracking was equal to 1.09, Fig. 7 (curve 1).

For the welded joint, decreasing in relative elongation compared to air by 9% (from 18.7 to 17.1%) was observed, Fig.4. The relative narrowing practically did not change (Table 4), the coefficient of susceptibility to stress-corrosion cracking was equal to 1.0, Fig.7 (curve 2). The nature of destruction, as in air and under corrosion potential, is viscous, the diameter of holes is larger and their depth is smaller, Fig. 5, 6.

Table 4. Mechanical properties of X70 and welded joint in air and corrosion-mechanical properties in the NS4 model soil electrolyte at different potentials

Tabela 4. Mehanička svojstva X70 i zavarenog spoja na vazduhu i koroziono-mehanička svojstva u NS4 modelu elektrolita tla pri različitim potencijalima

Indicator name	Sample characteristic	Experimental conditions, polarization potential, V				
		Air	E_{cor}	-0,75	-0,95	-1,05
δ, %	Base metal	28.0	27.0	28,5	29.0	25.6
	Welded joint	18.7	15.5	17.1	14.3	18.7
S, мм^2	Base metal	14,8	15.2	15,4	15.6	15,9
	Welded joint	17.2	19.5	17.2	18.3	17.7
ψ, %	Base metal	53,1	49.3	48,7	48.0	47
	Welded joint	42.7	35.2	42.6	39.1	41.1
K_S	Base metal	-	1.07	1,09	1.11	1,13
	Welded joint	-	1.21	1.0	1.09	1.03

At the protective potential of -0.95 V, the viscous nature of the fracture is observed both for the base metal and for the welded joint, but some brittle part on the breaking surface appears. For X70 steel, the relative elongation compared to relative elongation the specimen in air increased by 3% (from 28.0 to 29.0%), Fig. 3, but the relative narrowing decreased by approximately 10% (Table 4), and the coefficient of susceptibility to stress-corrosion cracking was 1.11, Fig. 7 (curve 1). For the welded joint, decreasing in relative elongation by 23.5% (from 18.7 to 14.3%) was established, Fig. 3, relative narrowing by 8% (from 42.7 to 39.1%), the coefficient of susceptibility to stress-corrosion cracking was equal to 1.09,

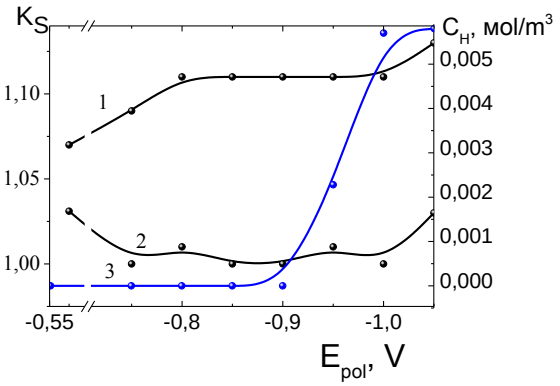

Figure 7. Tendency to stress-corrosion cracking of the base metal (1) and welded joint (2) of X70 steel and susceptibility of the steel to hydrogenation (3) at different potentials

Slika 7. Sklonost naponsko-korozionom pucanju osnovnog metala (1) i zavarenog spoja (2) čelika X70 i podložnost čelika hidrogenaciji (3) pri različitim potencijalima

Fig. 7 (curve 2). The fracture surface of the base metal is characterized by decreasing in the size of the fracture holes and the appearance of flat areas (Fig. 5), along which the rupture occurred. A similar nature of the rupture was observed for the welded joint, but visually larger proportion of flat areas can be noted, Fig. 6.

At the maximum protective potential -1.05 V for the base metal of X70 steel, the relative elongation decreased by 9% (from 28.0 to 25.6%), the relative contraction decreased by 4% (from 42.7 to 41.1%), Table 4, in the destruction the fragile character prevails, Fig. 5. The coefficient of susceptibility to stress-corrosion cracking is 1.13, Fig. 7 (curve 1). The indicator of relative elongation did not change and amounted to 18.7%, the relative narrowing of the welded joint decreased by 4%, to 41.1%. Part of flat areas in the destruction surface also prevails, Fig. 6. Susceptibility to stress-corrosion cracking coefficient K_S is 1.03, Fig. 7 (curve 2).

3.4. Study of propensity of X70 steel to electrolytic hydrogenation

The propensity of the base metal of X70 steel to electrolytic hydrogenation in NS4 model soil electrolyte was investigated according to Devanathan-Stakhursky method [26]. It was established that the dependence of the concentration of hydrogen penetrating through the steel membrane under cathodic polarization on the polarization potential is nonlinear. The penetration of hydrogen begins at a potential of -0.95 V, its concentration in steel is 0.0023 mol/m^3, and further increases at a potential -1.05V to 0.000518 mol/m^3, Fig. 7 (curve 3).

4. DISCUSSION OF THE RESULTS

According to the results of studies of X70 steel and welded joint, it was established that susceptibility to SCC of X70 steel itself, estimated by the K_S coefficient, increases when the potential changes from the corrosion potential to the minimum protective potential -0.75V slightly, from

1.07 to 1.09. This corrosion-mechanical behavior correlates with the tendency of steel to hydrogenation: in the NS4 solution, at potentials more positive than -0.75V, hydrogen penetration into X70 steel is not observed, Fig. 7 (curve 3). In the normalized DSTU 4219 range of protective potentials from -0.75 to -1.05V, more significant increasing in hydrogen penetration was noted, starting at the potential -0,95V. At the same time, the susceptibility to SCC changes non-monotonically: it almost does not increase up to potential of -0.95V and increases sharply from the potential -0.95 to -1.05V, i.e. K_S coefficient increases from 1.11 to 1.13, Fig. 7, curve 1. It can be assumed that this is caused by shifting in the equilibrium of cracking process and changing in its mechanism from local anodic dissolution to hydrogen embrittlement. At the potential -1.05 V, at which the concentration of hydrogen, penetrating through the steel changes abruptly from 0.002 mol/m^3 to 0.006 mol/m^3, the susceptibility to stress-corrosion cracking continues to increase, K_S increases up to 1.13.

For welded joint, the susceptibility to stress corrosion cracking in the range of potentials from the corrosion potential to the potential of -0.95 V, estimated by the K_S coefficient is lower than for the base metal, its values change little; it fluctuates around the value of 1.0. For the welded joint, no stable trend towards an increasing in susceptibility to stress-corrosion cracking with increasing (by absolute value) of polarization potential was found, Fig. 7, curve 2. Analyzed the macro- and microcuts of the samples of welded joints, was found that all of them were destroyed through the base metal, Fig. 8.

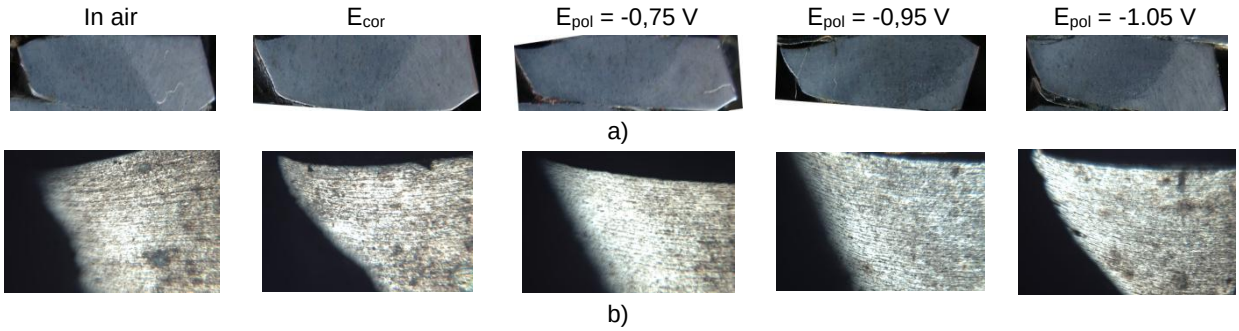

Figure 8. Fragments of the welded joint of X70 steel specimens breaking after corrosion-mechanical tests in air and in NS4 solution under different conditions: a - macrocuts, b - microcuts, ×100
Slika 8. Fragmenti zavarenog spoja čeličnih uzoraka X70 koji se lome nakon koroziono-mehaničkih ispitivanja na vazduhu i u rastvoru NS4 pod različitim uslovima: a - makrorezi, b - mikrorezovi, x100

Obtained results correlate satisfactorily with the results of the experience of analyzing cases of stress-corrosion cracking on main gas pipelines. It should be recalled that stress-corrosion cracks form and develop along the main metal on pipe of main gas pipelines. This is quite natural, since the quality of the weld and the indicators of the mechanical properties of the welded joint must comply with the construction standards of SNiP 2.05.06 and SNiP III-42-80, according to which poor weld formation is unacceptable.

Another important conclusion emerges from the obtained patterns of stress-corrosion cracking of the welded joint of X70 steel. Since the break is spread along the base metal, the proposed coefficient of susceptibility to stress-corrosion cracking K_S can be legitimately used for estimating of welded joint, provided the weld is performed in a high-quality manner.

5. CONCLUSIONS

1. X70 steel, studied in this work, has ferrite-pearlite structure with grain elongation in the rolling direction. The microstructure of the metal of the external seam of the welded joint is dispersed acicular ferrite with intergranular pre-eutectoid ferrite in the amount of no more than 6%. In heat affected zone on the area of coarse grain, the structure is bainite type with formations of polygonal pre-eutectoid ferrite formations on the boundaries of the past austenite grains. The size of the coarse grain in the heat affected zone in the area adjacent to the fusion line, has number 4.

2. According to the results of electrochemical studies, it was established that the corrosion potential of the weld seam is more positive than that for the base metal of X70 steel, and difference between corrosion potentials of the base metal and weld seam is 12 mV, which, according to GOST 9.005, does not represent danger and can be expected not to lead to overwhelming weld corrosion. The slope of anodic curve of the base metal is 0.057 V, the weld seam is 0.038 V, which confirms the diffusion control of the corrosion process. Electrochemical corrosion of the weld seam is inhibited compared to the base metal, probably due to passivation of surface by alloying elements in the seam.

The limiting oxygen reduction current on the base metal is 1.3 times less than on the weld, and the hydrogen reduction potential on the weld is slightly lower in absolute value compared to the base metal, which can create conditions for preferential hydrogenation of the weld area.

3 Hydrogen penetration through X70 steel membrane begins at potential -0.95V, its concentration in the steel is 0.0023 mol/m^3, and increases at potential of -1.05V to 0.000518 mol/m^3.

4. The tendency to stress-corrosion cracking of the base metal of X70 steel, estimated by K_S coefficient, increases when the potential changes from the corrosion potential to minimum protective potential -0.75V slightly, from 1.07 to 1.09, then K_S almost does not change up to potential -0.95V and sharply increases from the potential -0.95 to -1.05 V, from 1.11 to 1.13.

5. For welded joint, the K_S coefficient is lower than for the base metal, its values change a little, from 1.0 to 1.21. It was established that the rupture of the welded joint occurs along the base metal, which allows to propose stress-corrosion cracking susceptibility factor K_S to be legitimately used for the welded joint, provided the weld is performed in a high-quality manner.

Acknowledgements

This work was performed with financial support of E.O. Paton Electric Welding Institute of National Academy of Sciences of Ukraine (State registration number 0110U001621).

6. REFERENCES

[1] Z.Li, B.Sun, Q.Liu, Y.Yu, Z.Liu (2021) Fundamentally understanding the effect of Non-stable cathodic potential on stress corrosion cracking of pipeline steel in Near-neutral pH solution, *Construction and Building Materials*, *288*, 123117.

[2] Y.Z.Jia, J.Q.Wang, E.H.Han, W.Ke (2011) Stress corrosion cracking of X80 pipeline steel in near-neutral pH environment under constant load tests with and without preload, *Journal of Materials Science & Technology*, *27*(11), 1039-1046.

[3] H.Wan, D.Song, Z.Liu, C.Du, Z.Zeng, Z.Wang, X.Li (2017) Effect of negative half-wave alternating current on stress corrosion cracking behavior and mechanism of X80 pipeline steel in near-neutral solution, *Construction and Building Materials*, *154*, 580-589.

[4] H.Wan, D.Song, Z.Liu, C.Du, Z.Zeng, X.Yang, X.Li (2017) Effect of alternating current on stress corrosion cracking behavior and mechanism of X80 pipeline steel in near-neutral solution, *Journal of Natural Gas Science and Engineering*, *38*, 458-465.

[5] J.Q.Wang, A.Atrens (2003) SCC initiation for X65 pipeline steel in the “high” pH carbonate/ bicarbonate solution, *Corrosion Science*, *45*(10), 2199-2217.

[6] A.Egbewande, W.Chen, R.Eadie, R.Kania, G.Van Boven, R.Worthingham, J.Been (2014) Transgranular crack growth in the pipeline steels exposed to near-neutral pH soil aqueous solutions: discontinuous crack growth mechanism, *Corrosion Science*, *83*, 343-354.

[7] F.M.Song (2009) Predicting the mechanisms and crack growth rates of pipelines undergoing stress corrosion cracking at high pH, *Corrosion science*, *51*(11), 2657-2674.

[8] Z.Y.Liu, X.G.Li, Y.F.Cheng (2012) Mechanistic aspect of near-neutral pH stress corrosion cracking of pipelines under cathodic polarization, *Corrosion Science*, *55*, 54-60.

[9] W.Zheng, R.W.Revie, G.Shen, R.Sutherby, W.R.Tyson (2000) *Stress Corrosion Cracking of Linepipe Steels in Near-Neutral pH Environment: A Review of the Effects of Stress*, ASTM International.

[10] B.A.Kim, W.Zheng, G.Williams, M.Laronde, J.A.Gianetto, G.Shen, Y.Hosokawa (2004) Experimental study on SCC susceptibility of X60 steel using full pipe sections in near-neutral pH environment. In *International Pipeline Conference,* 41766, 133-141.

[11] J.Shimamura, D.Izumi, S.Igi, N.Ishikawa, S.Ueoka, K.Ihara, J.Kondo (2020) Material Design for Grade X65 UOE Sour Linepipe Steels with SSC-resistant Property, *International Journal of Offshore and Polar Engineering*, *30*(04), 487-492.

[12] A.Carmona-Hernandez, R.Orozco-Cruz, E.Mejía-Sanchez, A.Espinoza-Vazquez, A.Contreras-Cuevas, R.Galvan-Martinez (2021) Study of SCC of X70 Steel Immersed in Simulated Soil Solution at Different pH by EIS, *Materials*, *14*(23), 7445.

[13] Z.Cui, Z.Liu, L.Wang, X.Li, C.Du, X.Wang (2016) Effect of plastic deformation on the electrochemical and stress corrosion cracking behavior of X70 steel in near-neutral pH environment, *Materials Science and Engineering: A*, *677*, 259-273.

[14] P.Liang, C.W.Du, X.G.Li, X.Chen (2009) Effect of hydrogen on the stress corrosion cracking behavior of X80 pipeline steel in Ku'erle soil simulated solution, *International Journal of Minerals, Metallurgy and Materials*, *16*(4), 407-413.

[15] L.Zhiyong, C.Zhongyu, L.Xiaogang, D.Cuiwei, X.Yunying (2014) Mechanistic aspect of stress corrosion cracking of X80 pipeline steel under non-stable cathodic polarization, *Electrochemistry communications*, *48*, 127-129.

[16] H.Yuan, Z.Liu, X.Li, C.Du (2017) Influence of applied potential on the stress corrosion behavior of X90 pipeline steel and its weld joint in simulated solution of near neutral soil environment, *Jinshu Xuebao/Acta Metallurgica Sinica*, *53*(7), 797-807.

[17] Z.Y.Liu, C.W.Du, C.Li, F.M.Wang, X.G.Li (2013) Stress corrosion cracking of welded API X70 pipeline steel in simulated underground water, *Journal of materials engineering and performance*, *22*(9), 2550-2556.

[18] J.Luo, S.Luo, L.Li, L.Zhang, G.Wu, L.Zhu (2019) Stress corrosion cracking behavior of X90 pipeline steel and its weld joint at different applied potentials in near-neutral solutions, *Natural Gas Industry B*, *6*(2), 138-144.

[19] Q.L.Sun, B.Cao, Y.S.Wu (2008) Stress Corrosion Cracking of Weld Joint of Pipeline Steel X70 in

Near-Neutral Solution. *Transactions of Materials and Heat Treatment*, 39(3),125-129.
[20] Q.L.Sun, W.W.Shao, X.G.Wang, C.B.Wang (2013) Influence of Fluctuation Frequency on Stress Corrosion Cracking of X70 Pipeline Steel Welding Joint, In *Advanced Materials Research* (690, 2668-2672). Trans Tech Publications Ltd.
[21] B.Lu, J.L.Luo, D.G.Ivey (2010) Near-neutral pH stress corrosion cracking susceptibility of plastically prestrained X70 steel weldment, *Metallurgical and Materials Transactions A*, *41*(10), 2538-2547.
[22] S.G.Polyakov, A.A.Rybakov (2009) The main mechanisms of stress corrosion cracking in natural gas trunk lines, Strength of Materials, 41(5), 456–463
[23] R.A.deSena, I.N.Bastos, G.P.Mendes (2012) Theoretical and Experimental Aspects of the Corrosivity of Simulated Soil Solutions, *International Scholarly Research Notices,* Article ID 103715, p.6.
[24] L.I.Nyrkova, A.O.Rybakov, S.O.Osadchuk, S.L. Melnichuk, N.O.Hapula (2014) Device for investigation of sensibility of pipe steels to stress-corrosion cracking. Patent for invention, No 107229.
[25] L.I.Nyrkova, P.E.Lisovyi, L.V.Goncharenko, S.O. Osadchuk, V.A.Kostin, A.V.Klymenko (2021) Regularities of Stress-Corrosion Cracking of Pipe Steel 09G2S at Cathodic Polarization in a Model Soil Environment, *Physics and chemistry of solid state,* 22(4), 828 – 836.
[26] GOST R 9.915-2010 Unified system of corrosion and ageing protection. Metals, alloys, coatings, products. Test methods of hydrogen embrittlement.
[27] DSTU 8972:2019 Steel and alloys. Methods for detection and determination of grain size.
[28] GOST 9.005-72 Unified system of corrosion and ageing protection. Metals, alloys, metallic and non-metallic coatings. Permissible and impermissible contacts with metals and non-metals.
[29] L.Nyrkova (2020) Stress-corrosion cracking of pipe steel under complex influence of factors, *Engineering Failure Analysis,* 116, 104757.
[30] L.I.Nyrkova, S.O.Osadchuk, A.O.Rybakov, S.L. Mel'nychuk (2020) Methodical approach and a criterion for the evaluation of the susceptibility of pipe steel to corrosion cracking, *Materials Science,* 55(5), 625–632.
[31] L.I.Nyrkova, S.M.Prokopchuk, L.V.Goncharenko, S.O.Osadchuk (2021) Corrosion and mechanical behavior of 17G1S-U pipeline steel and its weld joint of in the terms simulating operational conditions, Journal of Physics: Conference Series, 2045(1), 012022.
[32] L.I.Nyrkova, P.E.Lisovoy, L.V.Goncharenko, S.O. Osadchuk, A.V.Klimenko, Yu.V.Borisenko, O.V. Batochkin (2021) Regularities of stress corrosion cracking of 10G2FB pipeline steel in near neutral soil environment at cathodic polarization, *Technologies and Engineering*, 2, 29-39.

IZVOD

ISTRAŽIVANJE NAPONSKO-KOROZIJSKOG PRSKANJA ZAVARENOG SPOJA ČELIKA X70 PRI KATODNOJ POLARIZACIJI U BLISKO NEUTRALNOJ SREDINI

Izvršeno je istraživanje naponsko-korozionog pucanja zavarenih spojeva od čelika X70 pri katodnoj polarizaciji u skoro neutralnom rastvoru NS4. Utvrđeno je da se sklonost osnovnog metala čelika X70 ka naponsko-korozionom pucanju, procenjena koeficijentom K_S, povećava sa 1,07 na 1,13, dok se polarizacioni potencijal menja od potencijala korozije do maksimalnog zaštitnog potencijala -1,05V. Ovakva pravilnost je u korelaciji sa povećanjem prodora vodonika kroz čelik X70, koji je pri maksimalnom zaštitnom potencijalu -1,05V jednak 0,000518 mol/m3. Podložnost zavarenog spoja je manja od osnovnog metala, promena K_S koeficijenta nije mnogo blizu vrednosti 1,0. Sa povećanjem potencijala polarizacije sa -0,75 V na -1,05 V površina loma čelika X70 karakteriše smanjenje veličine rupa i pojava ravnih površina, kroz koje je došlo do loma. Slična priroda rupture je primećena i za zavareni spoj, ali se može primetiti vizuelno veći udeo ravnih površina. Utvrđeno je da do pucanja zavarenog spoja dolazi na osnovnom metalu, što omogućava da se predloži faktor osetljivosti na naponsku koroziju K_S koji bi se legitimno koristio za procenu pucanja zavarenog spoja od naponske korozije, pod uslovom da je zavar izveden na visoko kvalitetan način. Rezultati prslina od naponske korozije zavarenog spoja čelika X70 zadovoljavajuće koreliraju sa iskustvom prslina od naponske korozije na magistralnim gasovodima, gde se prsline od naponske korozije formiraju i razvijaju duž osnovnog metala gasovoda.

Ključne reči: *čelik za cevi X70, zavareni spoj, skoro neutralna sredina, katodna polarizacija, naponsko-koroziono pucanje, deformacija, voltametrija, fraktografija*

Naučni rad
Rad primljen: 20. 08. 2022.
Rad prihvaćen: 29. 09. 2022.
Rad je dostupan na sajtu: www.idk.org.rs/casopis